Polyhedron 30 (2011) 2884–2889

Contents lists available at SciVerse ScienceDirect

Polyhedron

journal homepage: www.elsevier.com/locate/poly

Synthesis, characterization and crystal structures of the boratranes: 2,10,11-trioxa-6-aza-1-boratricyclo[4.4.4.0^{1,6}] tetradecane (tri-*n*-propanolamine borate), and 3-(4-methoxy)phenoxymethyl-7,10-dimethyl-2,8,9-trioxa-5-aza-1-boratricyclo[3.3.3.0^{1,5}]-undecane

Robert A. Franich [a,*], Brian K. Nicholson [b], Hank W. Kroese [a], Suzanne S. Gallagher [a], Roger Meder [c], Joseph R. Lane [b], Brian D. Kelly [d]

[a] Scion, Te Papa Tipu Innovation Park, 49 Sala Street, Rotorua 3020, New Zealand
[b] Chemistry Department, University of Waikato, Hamilton, New Zealand
[c] CSIRO Plant Industry, QBP, 306 Carmody Road, St. Lucia, Queensland 4067, Australia
[d] Starpharma Holdings Pty Ltd., 75 Commercial Road, Melbourne, Victoria 3004, Australia

ARTICLE INFO

Article history:
Available online 5 September 2011

Keywords:
Boratranes
X-ray crystal structure
N → B transannular bond length
Quantum chemical calculations

ABSTRACT

The crystal structures of boratranes 2,10,11-trioxa-6-aza-1-boratricyclo[4.4.4.0^{1,6}] tetradecane (tri-*n*-propanolamine borate) **1** as the tri-hydrate, and 3-(4-methoxy)phenoxymethyl-7,10-dimethyl-2,8,9-trioxa-5-aza-1-boratricyclo[3.3.3.0^{1,5}]-undecane **2** as the partial (0.2) hydrate have been determined. Compound **1** has a near-tetrahedral coordination of both the N (108.8°) and B atoms (111.2°), N → B bond length 1.656 Å and all-chair tricyclic conformation, whereas **2** has a slightly-longer N → B dative bond length (1.667 Å) and the O–B–O angle, 114.8°, was slightly distorted from near-tetrahedral to adopt a flatter conformation. Theoretical calculations on **1** and **2** showed that the B–N distance in each shortened markedly between isolated gas phase molecules and 'solvated' models. Neither structural results, nor calculated parameters, were able to explain the propensity towards slow hydrolysis of boratranes with five-membered rings compared with the relative hydrolytic stability of boratranes with six-membered rings.

1. Introduction

Boratranes are a class of tricyclic boric acid esters which have been known since the description of the simplest example prepared using triethanolamine in 1951 [1]. The particular structural feature of boratranes, which explains their stability towards hydrolysis [2,3], is the *trans*-annular nitrogen-to-boron dative bond, imparting tetrahedral geometry to the N and B atoms, described as a 'tryptych' structure. This structural motif is common to numerous synthetic compounds collectively referred to as 'atranes', the chemistry of which has been extensively reviewed [4].

Boric acid is well-known as a broad-spectrum biocide which has found economic application for the protection of wood from fungal decay and wood-boring insects [5]. This benefit of wood protection has historically been limited to products used in the interior of buildings, or protected from rain because boric acid and borate salts are soluble in water, and therefore leach from wood when wet over a period of time [6], eventually leaving the wood susceptible to decay. Many attempts have been made to limit the rate of leaching of boron element from treated wood [7]. One approach to solving this problem has exploited the valence-shell electron-pair deficiency of boron (relative to the neon octet), and involved the synthesis and biocidal effectiveness testing of molecules where the boron atom was coordinated to nitrogen by an electron-pair dative bond, such as in biguanide complexes [8,9] and in boratranes [10]. The *in vitro* fungicidal performance of the variety of boratranes synthesised [10] was found to be dependent on atrane ring-size, where those with six-membered rings, e.g., tri-*n*-propanolamine borate **1** and its C-substituted derivatives [10], had lower fungicidal effectiveness compared with those boratranes having five-membered rings, e.g., triethanolamine borate and its C-substituted alkyl and aryl derivatives, such as **2**. This may be attributed to the observation that while five-membered ring boratranes hydrolyzed slowly to release boric acid, the six-membered species were indefinitely stable towards water at neutral pH [10].

Hydrolysis of boratranes has been shown to be dependent on the ability of a water molecule to attack the boron atom to form an S_N2-type transition state leading to a partially-hydrolyzed intermediate structure, as part of a step-wise formation of boric acid and the corresponding alkanolamine [2,3]. Closeness of approach of the water nucleophile to the boron atom would depend on both

* Corresponding author.
E-mail address: Robert.Franich@scionresearch.com (R.A. Franich).

0277-5387/$ - see front matter © 2011 Elsevier Ltd. All rights reserved.
doi:10.1016/j.poly.2011.08.020

steric factors (e.g., accessibility of the boron atom within the 'tryptych' structure, related to the O–B–O bond angles), and electronic factors, (molecular orbital and dipole moment). With simple alkyl-substituted boratranes, such as tri-*iso*-propanolamine borate, the hydrolysis rate of the boratrane was considered to be related to the length of the N → B dative bond and distortions from the ideal tetrahedral bond angles around the N and B atoms as a result of steric interactions between the alkyl substituents [2,3].

In the classical, acyclic donor-acceptor complexes of boron trifluoride and borane with ammonia and alkylamines, the N → B bond lengths and bond angles have been determined from both experimental (X-ray crystallography and gas-phase microwave spectroscopy) and theoretical quantum mechanical calculations [11]. The N → B bond length was found to be shorter in the crystal (e.g., for $H_3N \rightarrow BH_3$, 156.4 Å) than in the gas phase, 165.7 Å [11], and bond angles close to those of tetrahedral coordinate B and N atoms. Large-ring boron-amine complexes, such as with porphine and porphyrin ligands [12,13] also have N → B bond lengths in the range 1.54–1.60 Å, and bond angles close to tetrahedral N and B coordination, determined by X-ray crystallography. Small-ring, highly-strained boron–amine complexes have much-shortened (e.g., 1.375 Å) N → B bond lengths [14].

Whereas N → B bond lengths determined by X-ray crystallography represent the molecular structure in its solid state, in solution the N → B bond is dynamic, lengthening in the presence of nucleophiles which approach the B atom in an S_N2-type mechanism. An example displaying this in a crystal structure is a 2,6-bis(*N*,*N*-dimethylaminomethyl)phenylboronate ester, where the N → B bond length is stretched to 1.762 Å and the bond angles (116–121°) around the B atom are flattened close to trigonal coordination, as would be expected in an S_N2-type transition state [15].

There are few published X-ray crystal structures of boratranes. The simplest, triethanolamine borate (referred to as 'boratrane' in the literature) was shown to have an N → B bond length of 1.655 Å [16,17]. This contrasts with the N → B bond length, 1.846 Å, determined in the gas phase by electron diffraction [18,19]. A crystalline derivative of triethanolamine borate with two phenyl rings on the C atoms of one ring has a N → B bond length of 1.685 Å [20]. Crystal structures of methyl-substituted five-membered ring boratranes have been recently reported, with N → B bond-lengths of 1.663 Å for the hexamethyl-, and 1.684 Å for the tetramethyl-derivative [21]. The structure of the six-membered ring boratrane, tri-*n*-propanolamine borate **1** has been reported [22], but was derived from visually-estimated photographic data ($R_1 = 0.12$), and with no coordinates published. A more precise structure determination was therefore undertaken, and reported here, as the only example of a six-membered ring system boratrane for which X-ray crystallographic data have been obtained. Among the various water-insoluble C-substituted five-membered ring system boratrane compounds synthesised as candidate wood protection chemicals [10], few formed crystals suitable for X-ray study. One compound, **2** (Fig. 1) did give suitable crystals and the structure of this boratrane is also reported.

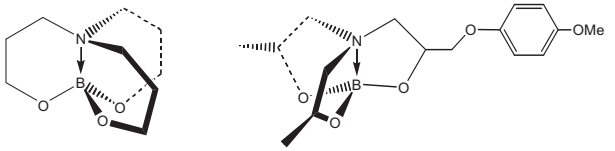

(**1**) (**2**)

2,10,11-trioxa-6-aza-boratricyclo [4.4.4.$0^{1,6}$]-tetradecane

3-(4-methoxy)phenoxymethyl-7,10-dimethyl-2,8,9-trioxa-5-aza-1-boratricyclo[3.3.3.$0^{1,5}$]-undecane

Fig. 1. Molecular structures and systematic names for compounds **1** and **2**.

Fundamental knowledge of the structural features of the boratranes described in this paper, and relating these to the compound hydrolysis rates has enabled a rational approach to design, synthesis and formulation for practical application of wood protection chemicals based on substituted five-membered ring boratranes.

2. Experimental

2.1. Materials and methods

All chemicals and reagents were from Sigma–Aldrich and were used as received. Infrared (IR) spectroscopy was carried out using a Bruker Vector 33 spectrometer using samples prepared as KBr discs. Nuclear magnetic resonance (NMR) spectroscopy was carried out in $CDCl_3$ solution using a Bruker Avance DPX400 instrument operating at 100.13 MHz for ^{13}C, 400.13 MHz for ^{1}H and 128.38 MHz for ^{11}B nuclei, relative to external standard BH_4^- at 0 ppm chemical shift. Gas chromatography–mass spectrometry (GC–MS) was carried out using an Agilent 5790 instrument fitted with a 30 m × 0.2 mm HP5 fused-silica capillary column and helium as the carrier gas at 1 mL min^{-1} flow rate using a temperature program from 40–280 °C at 4 °C/min. Spectra were acquired in electron ionization mode at 70 eV, 300 μA electron energy, and are reported as *m*/*z* mass-to-charge ratio and intensity relative to the spectrum base peak.

2.2. Preparation and characterization of the boratranes **1** and **2**

2.2.1. Synthesis of 2,10,11-trioxa 6-aza-1-boratricyclo[4.4.4.$0^{1,6}$] tetradecane (**1**)

Tris(propan-3-ol)amine was prepared by $LiAlH_4$ reduction of *tris*(2-carbethoxyethyl)amine, itself prepared by Michael addition of liquid anhydrous ammonia to ethyl acrylate [23]. To *tris*(propan-3-ol)amine (19 g, 0.1 mol) placed in a round-bottomed flask was added toluene (100 mL) and boric acid (6.18 g, 0.1 mol) and the mixture was stirred and heated under a Dean-Stark water separator until the theoretical volume of water had been collected. The solution was cooled, filtered from a small quantity of residue, and concentrated to give a white solid. A concentrated solution of this solid was made in boiling 95% ethanol, which was allowed to gradually cool. Crystals of **1** deposited as needles which were isolated by filtration and dried at ambient temperature *in vacuo*. GC–MS analysis of **1** showed a single peak at 42.85 min retention time.

M.p. 248 °C IR (cm^{-1}) 3420 (OH, water of crystallization), 2956, 2927, 2883 (CH_2 str.), 1257 (B–O str.), 592 (N–B str.).

^{1}H NMR (ppm) 2.03 (m, 6H, $-CH_2-$), 4.0 (t, 6H, $N-CH_2-$), 5.09 (m, 6H, $O-CH_2-$). ^{13}C NMR (ppm) 23.6 ($-CH_2-$), 54.1 ($N-CH_2-$), 61.4 ($O-CH_2-$). ^{11}B NMR (ppm) 0.2 GC–MS (*m*/*z*) 199 ($M^{+\cdot 11}B$), 198 ($M^{+\cdot 10}B$), 140 (100%), 82 (61%), 57 (63%), 42 (64%).

2.2.2. Synthesis of 3-(4-methoxy)phenoxymethyl-7,10-dimethyl-2,8,9-trioxa-5-aza-1-boratricyclo[3.3.3.$0^{1,5}$]-undecane (**2**)

To racemic 3-(4-methoxy)-phenoxypropan-1,2-oxirane (1.8 g, 0.01 mol) was added di-*iso*-propanolamine (1.33 g, 0.01 mol) and a few small crystals of toluene-*p*-sulfonic acid. The mixture was stirred and heated without solvent at 60 °C for 5 h. The crude alkanolamine product was added to toluene (50 mL) in a round-bottomed flask, and boric acid (0.62 g, 0.01 mol) was added. The mixture was stirred and heated under Dean-Stark water separation conditions until the theoretical volume of water had been obtained. The cooled solution was filtered, and then concentrated to give a white solid. A portion of the crude boratrane product was dissolved in hot 95% ethanol, allowed to cool and to crystallise. The needle-shaped crystals were filtered and dried at ambient temperature *in vacuo*. GC–MS

of crystalline **2** showed three peaks with retention time 44.53, 44.83 and 45.31 min, and in the area% ratio of 0.40:0.13:0.47, respectively. The mass spectra for all three GC–MS peaks were nearly identical.

M.p. 152–153° IR (cm^{-1}) 3440 (OH, water of crystallization), 3080 (Ar–H str.), 2972, 2910, 2865 (CH_2 str.), 1513 (Ar C=C str.), ^{1}H NMR (ppm) 1.18 (d, J = 7 Hz, 6H, CH_3), 3.26 (dd, J = 7 Hz, 3H, NCH_2), 3.51 (dd, J = 7 Hz, 3H, NCH_2), 3.83 (s, 3H, $ArOCH_3$), 3.95 (m, 3H, $ArOCH_2$, C*H*-CH_3), 4.3 (m, 1H, CH_2–CH–O), 6.9 (s, 4H, ArH). ^{13}C NMR (ppm) 24.0 (CH_3), 45.0, 51.8 (N–CH_2), 54.1, 57.1 (O–CH), 55.9 (OCH_3), 72.7 (O–CH_2), 114.8 115.3, 151.6, 152.2 (ArC). ^{11}B NMR (ppm) 12.0 GC–MS (m/z) 321 ($M^{+\cdot 11}$B), 320 ($M^{+\cdot 10}$B), 198 (100%), 197 (20%), 184 (82%), 183 (16%), 154 (44%), 140 (35%), 123 (49%).

2.3. X-ray crystallography

Crystals of **1** were determined as the trihydrate, $N\{(CH_2)_3O\}_3B{\cdot}3H_2O$, while those of **2**, were determined as the partial hydrate. X-ray intensity data were obtained from a Bruker APEX II CCD diffractometer with MoKα radiation (0.71073 Å), and were processed using standard software. Corrections for absorption were carried out using SADABS [24]. The structures were solved and refined (on F_o^2) using the SHELX programs [25,26], operating under WinGX [27,28]. For **1**, Freidel equivalents were merged, and H atoms were included in calculated positions except for those of the water molecules which were located and refined with fixed temperature factors. For **2**, a final peak of residual electron density was assigned as a water molecule in the lattice, disordered over two symmetry equivalent sites with occupancy about 0.2. This is weakly H-bonded to O(2) and was included in the refinement without the associated H atoms.

2.4. Theoretical methods

The geometries of **1** and **2** were optimized using the B3LYP and M06-2x hybrid density functional methods, the B2PLYP and mPW2PLYP double hybrid density functional methods, the B2PLYPd and mPW2PLYPd dispersion corrected double hybrid density functional methods and the MP2 *ab initio* method. The 6-31G(d) and 6-311+G(2d,2p) Pople style basis sets, the cc-pVDZ, aug-cc-pVDZ and cc-pVTZ correlation consistent basis sets were used. The geometry of **1** and **2** with the MP2/6-31G(d) method in an aqueous environment was also optimized using the Integral Equation Formalism Polarisable Continuum Model (IEF-PCM) and calculated atomic charges using Natural Bond Orbital (NBO) analysis. The initial geometries were taken from the corresponding X-ray crystal structure. Harmonic vibrational frequencies were also calculated to verify that the optimized structures were true minima. All calculations were completed using GAUSSIAN 09, Revision A.01 [29].

3. Results and discussion

3.1. X-ray crystal structure determinations

Crystal data and refinement details for **1** and **2** are summarized in Table 1.

The structure of **1**, as the trihydrate, $N[(CH_2)_3O]_3B{\cdot}3H_2O$, showed the boratrane to lie on a three-fold axis of the chiral space group $R\bar{3}$, coincident with the N → B vector. The six-membered rings have adopted a chair conformation, as shown in Fig. 2. There is the expected N non-bonding electron pair interaction between the N and B atoms, with a distance of 1.656(2) Å, which compares with the sum of the covalent radii for the three-coordinate atoms of 1.61 Å, so can be regarded as a strong interaction. This also allows for near-ideal tetrahedral bonding at each of the atoms (O–B–O′ 111.19(6)°, C–N–C′ 108.76(6)°). The H_2O molecules in the lattice form an infinite H-bonded helical chain parallel to the c axis with the second hydrogen atom H-bonded to O of the boratrane.

Table 1
Crystal data and refinement details for the boratranes **1** and **2**.

	1	**2**
Formula	$C_9H_{24}BNO_6{\cdot}3H_2O$	$C_{16}H_{24}BNO_5{\cdot}0.2H_2O$
M_r	253.10	324.78
T (K)	89(2)	118(2)
Crystal system	trigonal	monoclinic
Space group	$R\bar{3}$	$P2_1/c$
a (Å)	13.6873(3)	16.9480(5)
b (Å)	13.6873(3)	5.5575(2)
c (Å)	5.9896(3)	17.9064(5)
β (°)		97.528(2)
V (Å^3)	971.77(6)	1672.04(9)
Z	3	4
D_{calc} (g cm^{-3})	1.297	1.290
μ (mm^{-1})	0.105	0.094
Crystal size (mm)	0.51 × 0.45 × 0.44	0.41 × 0.30 × 0.09
F(000)	414	696
θ_{max} (°)	27.5	30.2
Reflections collected	7352	42 513
$T_{max,\ min}$	0.95, 0.89	1.00, 0.90
Unique reflections	816 (R_{int} = 0.037)	4937 (R_{int} = 0.043)
R_1 [$I > 2\sigma(I)$]	0.0291	0.0517
wR_2 (all data)	0.0741	0.1610
Goodness-of-fit (GOF) on F^2	1.154	1.014

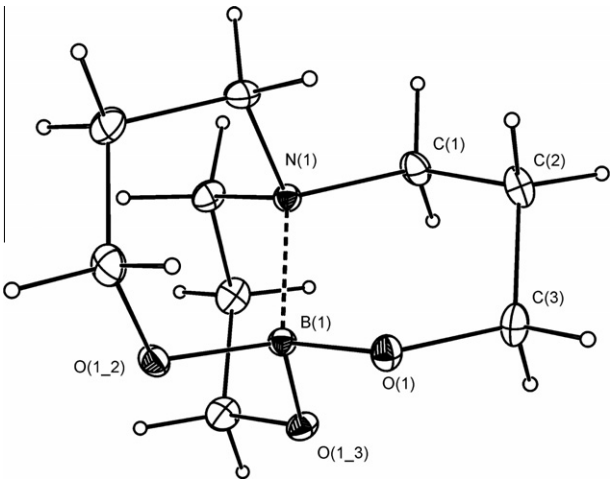

Fig. 2. Molecular structure of 12,10,11-trioxa-6-aza-1-boratricyclo[4.4.4.0^{1,6}] tetradecane **1**.

Other bond parameters for **1** are listed in Table 2.

The structure of 3-(4-methoxy)phenoxymethyl-7,10-dimethyl-2,8,9-trioxa-5-aza-1-boratricyclo[3,3,3,01,5]-undecane **2** is shown in Fig. 3, and is the first example of an X-ray crystal structure of an alkyl-substituted boratrane derived from di-*iso*-propanolamine. There are three five-membered rings which adopt an envelope conformation with the phenoxymethyl-substituted C atom being the out-of-plane component. For **2**, there was partial disorder in the conformation of the two methyl substituted rings involving C(4) and C(7), and this was modeled successfully. That the two methyl-substituted rings are partially disordered with minor components adopting the reverse conformation, as shown in Fig. 4, can be traced back to the original di-*iso*-propanolamine used in the synthesis consisting of a 1:1 mixture with methyl groups *syn* or *anti* to each other. The fact that the disorder is not 1:1 in the boratrane molecule analyzed showed there was some selectivity in the formation and crystallization of the *anti* stereoisomer, an interpretation supported from the GC–MS data acquired for the crystals and for the solid remaining in the mother liquor.

Table 2
Bond parameters for the six-membered ring (**1**) and the five-membered ring[a] (**2**) boratranes.

	(**1**)	(**2**)
Bond lengths (Å)		
N(1) → B(1)	165.6(2)	166.7(2)
N(1)–C(1)	150.5(10)	148.6(2)
C(1)–C(2)	151.6(15)	
C(2)–C(3)	151.2(16)	
C(3)–O(1)	142.4(13)	
O(1)–B(1)	144.0(8)	143.7(2)
Angles (°)		
C(1)–N(1)–C(1)′	108.76(6)	114.8(2)
O(1)–B(1)–O(1)′	111.19(6)	114.8(2)
B(1)–O(1)–C(3)	116.38(7)	109.2(2)
N(1)–C(1)–C(2)	112.74(8)	105.5(2)
C(1)–C(2)–C(3)	110.83(9)	

[a] Average values.

The N → B bond length of 1.667(2) Å is essentially the same as in the unsubstituted boratranes with five-membered rings [18,19]. This N → B bond length for **2** is slightly longer than that [1.656(2) Å] found for **1,** with six-membered rings, presumably because of less flexibility for the five-membered 'tryptych' rings. The extra rigidity (compared with **1**) is also manifested in distortion from the ideal tetrahedral bond angles, resulting in flattened geometry about the B and N atoms with bond angles (O–B–O (av.) 114.8°, C–N–C (av) 114.8° (Table 2)). The presence of a large substituent on one of the rings has little effect on the overall boratrane structure, though small changes would not be apparent because of the partial disorder in the methyl-substituted rings. The H_2O molecules in the lattice are disordered over two symmetry-equivalent sites which lie in channels parallel to the *b* axis, and are loosely H-bonded to the O(2) atom of the boratrane.

3.2. Quantum mechanical calculations

Data for the boratranes **1** and **2** modeled as isolated species using various levels of theory are summarized in Table 3. There is mostly reasonable agreement between calculated parameters and the ones determined from crystal structures, with the notable exception of the B–N distance where the calculated values are much longer than the experimental ones. Interestingly, the B3LYP result is very poor, especially for compound **1** (calc. 2.347 Å versus experimental 1.657 Å), despite this being the most widely-used density functional method. Better agreement is seen with the MP2/6-31G(d) method, but even here, the calculated value is ca. 0.1 Å longer. Earlier calculations for the unsubstituted five-membered ring boratrane reported the same lack of agreement for the B–N distance, and noted that the experimental values differed for the crystal structure value [1.6764(7) Å] and the gas phase electron diffraction result [1.84(4) Å] [18,19]. This suggested the molecular environment was having a significant effect on the B–N distance. To probe this further calculations on **1** were performed which included three water molecules (H-bonded to the O atoms as found in the crystal structure) and also for a dimer of **1** to partially account for other crystal packing interactions, with and without the water molecules. As shown in Table 4, by including the various HOH···O and C–H···O intermolecular interactions, better, though still not perfect, agreement is achieved. These intermolecular interactions withdraw electron density from the O atoms, which in turn make the B atom more electron deficient and hence attractive to the electron rich N atom. The structures were also optimized with the MP2/6-31G(d) method for an aqueous environment using implicit solvation, which gave calculated N → B distances of 1.709 and 1.691 Å for **1** and **2**, respectively. Both the X-ray and theoretical methods show that for these boratrane molecules interaction with polar neighbors has an unusually dramatic effect by shortening the N → B distance compared with that found by electron diffraction, or theory, for isolated gas phase molecules.

Table 3 also lists vibrational frequencies nominally assigned to the B–N stretching mode, though there is strong coupling with other ring motions. What the values do reflect is that the mode is at lower energy for the six-membered ring than for the five-membered one, arising no doubt from the greater flexibility. These results can be compared with a very recent theoretical study on five-membered ring group 13 atranes in general [30].

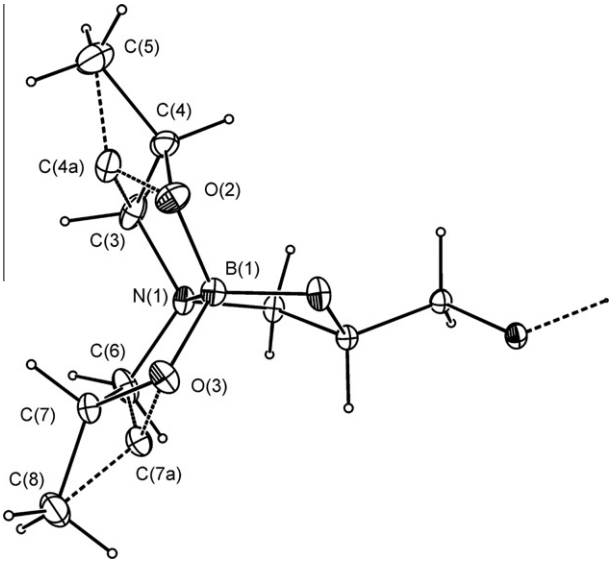

Fig. 4. Partial disorder of the two methyl-substituted rings in **2**.

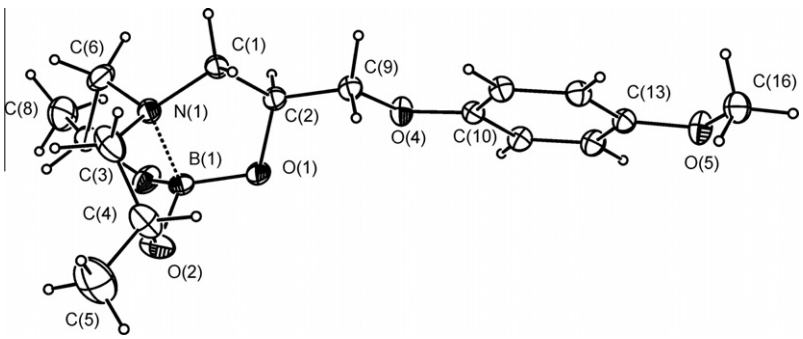

Fig. 3. Molecular structure of 3-(4-methoxy)phenoxymethyl-7,10-dimethyl-2,8,9-trioxa-5-aza-1-boratricyclo[3,3,3,$0^{1,5}$]-undecane **2**.

Table 3
Selected calculated and experimental data for **1** and **2**.

	B3LYP/6-31G(d)		M06-2x/6-31G(d)		MP2/6-31G(d)		Experimental	
	1	**2**	**1**	**2**	**1**	**2**	**1**	**2**
N–B bond length (Å)	2.347	1.828	1.816	1.805	1.774	1.758	1.656	1.667
O–B bond length (Å)	1.382	1.424	1.417	1.425	1.429	1.436	1.440	1.437
C–N–B angle (°)	106.8	101.0	108.6	142.3	109.1	102.1	110.2	103.3
N–B–O angle (°)	94.7	99.4	102.7	101.3	103.5	100.3	107.7	103.4
O–B–O angle (°)	119.3	117.4	115.3	117.4	114.7	116.9	111.2	114.8
Dipole moment (Debye)	3.457	7.086	5.026	7.239	5.680	8.335		
N–B stretch (cm^{-1})	220	343	298	459	325	488		

Table 4
Optimized N–B distance of **1** as both a monomer and dimer, and the corresponding hydrated monomer and dimer.

Method	N–B distance (Å)			
	Monomer	Monomer + $3H_2O$	Dimer	Dimer + $3H_2O$
B3LYP/6-31G(d)	2.347	1.810	1.883	1.781
B3LYP/cc-pVTZ	2.383	1.779	2.337	1.770
M062x/6-31G(d)	1.816	1.718	1.747	1.703
M062x/cc-pVTZ	1.802	1.712	1.746	1.709
MP2/6-31G(d)	1.774	1.704	1.736	1.703

3.3. Possible reasons for differing hydrolysis reactivities

The structure determinations were carried out partly with the expectation that the results would help understand the observation that the five-membered ring boratranes such as **2** hydrolyzed faster than the six-membered ones, **1** [2,3,10]. However, the new data have not provided clarity. A proposed mechanism for hydrolysis would involve nucleophilic attack by the O of a water molecule at the B atom, possibly aided by simultaneous H-bonding to one of the O atoms adjacent to the B atom to give a four-membered transition state, such as that shown in Fig. 5.

The X-ray crystal structure determinations for the boratranes **1** and **2** have shown only small differences in the N → B bond lengths between **1** and **2**, which means the earlier proposal that the rates of hydrolysis depend on the N → B interaction [2,3] does not appear to apply here. Another factor is the accessibility of the B atom to attack but space-filling models show that the boron atoms of both **1** and **2** are similarly exposed from within the 'tryptych' structure (Fig. 6). The B in the less readily-hydrolyzed **1** is slightly less exposed based on the O–B–O angle of 111.19(6)° compared with partly flattened 114.8(2)° for **2**, but the small difference is unlikely to be a major influence.

Electronic factors will also be involved, so partial atom charges were calculated. The MP2/6-31G(d) NBO charges for B are +1.48 for **1** and +1.49 for **2**, modeled in the aqueous phase. These showed that the residual +ve charge on the B atoms are not significantly different for **1** and **2**, so the different susceptibility to nucleophilic attack cannot be explained on that basis.

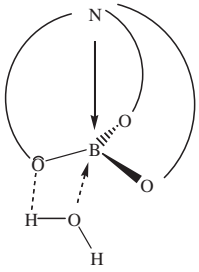

Fig. 5. A schematic for the attack of a H_2O molecule as the first step towards hydrolysis.

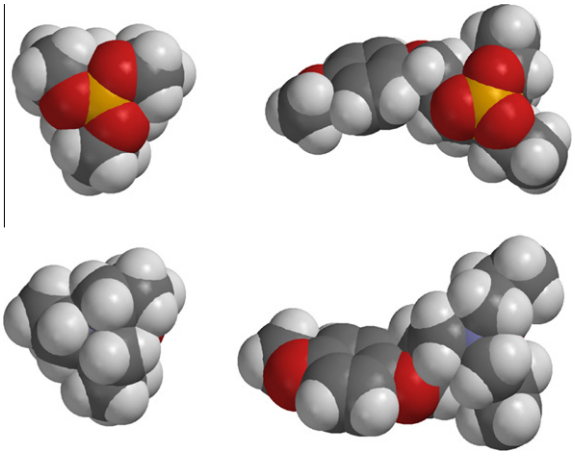

Fig. 6. Space-filling models of the six-membered ring (left) and five-membered ring boratranes showing very similar access to the B atom (orange), and different exposure of the N atom (blue). (For interpretation of the references to colour in this figure legend, the reader is referred to the web version of this article.)

A possible activating mechanism might involve protonation at the N atom, thus weakening the N → B interaction and increasing the reactivity at B. Protonation of the N atom of atranes by strong acids is documented [20]. However, examination of the molecular surface using space-filling models showed that the N atoms of both **1** and **2** are almost completely buried within the hydrophobic atrane cage (Fig. 6). For **2,** the N is a little more accessible [C–N–C′ angle 114.8(2)°] compared with **1** [C–N–C′ 108.8(1)°], which would allow **2** to be the more hydrolytically-reactive molecule, in agreement with the experimental results, but given the low energy of the N → B stretching vibration, this small difference in the ground state is again unlikely to have a major effect. The MP2/6-31G(d) NBO charges for the N atoms in **1** and **2** are −0.58 and −0.60 respectively which would indicate that **2** is slightly more basic than **1**, but the difference is barely significant.

This study of the structure and properties of five-membered ring boratranes represented by **2** and contrasting these with those of **1** attempts to understand at the molecular level the performance of such compounds as biocides for the protection of biomaterials, such as wood, against fungal decay. The pH of wood material when wet is in the range 4–6, and therefore a supply of protons would be available for bonding to N of a designed, water-insoluble C-substituted five-membered ring boratrane as a wood decay protectant, resulting in a controlled degree of hydrolysis and a slow-release of boric acid, on demand, as material moisture content varied. However, neither the X-ray results, nor the theoretical calculations, provide any compelling explanation for the different hydrolysis behavior of the boratranes. In the five-membered ring structure **2** there is a small but significant flattening away from the ideal tetrahedral coordination around both the B and N atoms, compared with the

six-membered **1**, taking both these atoms towards the hydrolysis reaction transition state geometry for S_N2 attack of H_2O at B, and protonation at N, respectively. However, whether these small ground-state differences account for the different hydrolysis rates is currently difficult to ascertain. More detailed calculations for the entire hydrolysis reaction pathways will be needed to resolve any differences in transition states between **1** and **2** to account for the differences in observed hydrolysis susceptibilities.

Acknowledgement

Dr. Jan Wikaira, University of Canterbury, Christchurch, New Zealand, is thanked for collection of the X-ray data.

Appendix A. Supplementary data

CCDC 809172 and 809173 contain the supplementary crystallographic data for compounds **1** and **2**. These data can be obtained free of charge via http://www.ccdc.cam.ac.uk/conts/retrieving.html, or from the Cambridge Crystallographic Data Centre, 12 Union Road, Cambridge CB2 1EZ, UK; fax: (+44) 1223-336-033; or e-mail: deposit@ccdc.cam.ac.uk.

References

[1] H.C. Brown, E.A.J. Fletcher, J. Am. Chem. Soc. 73 (1951) 2808.
[2] H. Steinberg, D.L. Hunter, J. Am. Chem. Soc. 82 (1960) 853.
[3] H. Steinberg, Organoboron Chemistry, John Wiley and Sons, NY, 1964, p. 855.
[4] J.G. Verkade, Coord. Chem. Rev. 137 (1994), p. 233.
[5] R. Cockroft, J.F. Levy, J. Inst. Wood Sci. 6 (1973) 28.
[6] K.M. Harrow, N.Z.J. Sci. Technol. 33 (1952) 471.
[7] A. Peylo, H. Willeitner, Holzforschung 49 (1995) 211.
[8] K.B. Anderson, R.A. Franich, H.W. Kroese, R. Meder, C.E.F. Rickard, Polyhedron 14 (1995) 1149.
[9] K.B. Anderson, R.A. Franich, H.W. Kroese, R. Meinhold, R. Meder, C.E.F. Rickard, Mater. Organ. 31 (1997) 63.
[10] R.A. Franich, Preservative Compounds and Their Use, 1997, NZ Patent 514356.
[11] V. Jonas, G. Frenking, J. Chem. Soc., Chem. Commun. (1994) 1489.
[12] W.J. Belcher, P.D.W. Boyd, P.J. Brothers, M.J. Liddell, C.E.F. Rickard, J. Am. Chem. Soc. 116 (1994) 8416.
[13] W.J. Belcher, M.C. Hodgson, K. Sumida, A. Torvisco, K. Ruhlandt-Senge, D.C. Ware, P.D. W Boyd, P.J. Brothers, J. Chem. Soc., Dalton Trans. (2008) 1602.
[14] A. Hergel, H. Pritzkow, W. Siebert, Angew. Chem., Int. Ed. Engl. 33 (1994) 1247.
[15] S. Toyota, T. Futawaka, H. Ikeda, M. Ōki, J. Chem. Soc., Chem. Commun. (1995) 2499.
[16] Z. Taira, K. Osaki, Inorg. Nucl. Chem. Lett. 7 (1971) 509.
[17] R. Mattes, D. Fenske, K.F. Tebbe, Chem. Ber. 105 (1972) 2089.
[18] I.F. Shishov, L.V. Khristenko, F.M. Rudakov, L.V. Vilkov, S.S. Karlov, G.S. Zaitseva, S. Samdal, J. Mol. Struct. 641 (2002) 199.
[19] A. Korlyukov, K.A. Lyssenko, M.Y. Antipin, N.V. Kirin, E.A. Chemyshev, S.P. Knyazev, Inorg. Chem. 41 (2002) 5043.
[20] S.S. Karlov, A.A. Selina, E.S. Chernyskova, Y.F. Oprunenko, A.A. Merkulov, V.A. Tafeenko, A.V. Churakov, J.A.K. Howard, G.S. Zaitseva, Inorg. Chim. Acta 360 (2007) 563.
[21] D.J. Kim, S.-D. Mun, S. Woo, C.H. Oh, H.-R. Park, T.-S. You, J. Lee, Y. Kim, Polyhedron 30 (2011) 1076.
[22] Z. Taira, K. Osaki, Inorg. Nucl. Chem. Lett. 9 (1973) 207.
[23] B.P. Devlin, D.A. Tirrell, Macromolecules 19 (1986) 2466.
[24] R.H. Blessing, Acta Crystallogr. A51 (1995) 33.
[25] G.M. Sheldrick, SHELX97 Programs for the Solution and Refinement of Crystal Structures, University of Göttingen, Germany, 1997.
[26] G.M. Sheldrick, Acta Crystallogr. A64 (2008) 112.
[27] L.J. Farrugia, WinGX Version 1.70.01, University of Glasgow, UK.
[28] L.J. Farrugia, J. Appl. Crystallogr. 32 (1999) 837.
[29] Gaussian 09, Revision A.02, M.J. Frisch, G.W. Trucks, H.B. Schlegel, G.E. Scuseria, M.A. Robb, J.R. Cheeseman, G. Scalmani, V. Barone, B. Mennucci, G.A. Petersson, H. Nakatsuji, M. Caricato, X. Li, H.P. Hratchian, A.F. Izmaylov, J. Bloino, G. Zheng, J.L. Sonnenberg, M. Hada, M. Ehara, K. Toyota, R. Fukuda, J. Hasegawa, M. Ishida, T. Nakajima, Y. Honda, O. Kitao, H. Nakai, T. Vreven, J.A. Montgomery, Jr., J.E. Peralta, F. Ogliaro, M. Bearpark, J.J. Heyd, E. Brothers, K.N. Kudin, V.N. Staroverov, R. Kobayashi, J. Normand, K. Raghavachari, A. Rendell, J.C. Burant, S.S. Iyengar, J. Tomasi, M. Cossi, N. Rega, N.J. Millam, M. Klene, J.E. Knox, J.B. Cross, V. Bakken, C. Adamo, J. Jaramillo, R. Gomperts, R.E. Stratmann, O. Yazyev, A.J. Austin, R. Cammi, C. Pomelli, J.W. Ochterski, R.L. Martin, K. Morokuma, V.G. Zakrzewski, G.A. Voth, P. Salvador, J.J. Dannenberg, S. Dapprich, A.D. Daniels, Ö. Farkas, J.B. Foresman, J.V. Ortiz, J. Cioslowski, D.J. Fox, Gaussian, Inc., Wallingford CT, 2009.
[30] A.K. Phukan, A.K. Guha, Inorg. Chem. 50 (2011) 1361.